View metadata, citation and similar papers at core.ac.uk

brought to you by CORE

provided by Arrow@dit

Technological University Dublin

ARROW@TU Dublin

Articles

School of Electrical and Electronic Engineering

2014

Photonic Crystal Fiber Half-Taper Probe Based Refractometer

Pengfei Wang
Technological University Dublin

Ming Ding
Optoelectronics Research Centre, University of Southampton,

Lin Bo
Technological University Dublin

Chunying Guan
Key Laboratory of In-fiber Integrated Optics of Ministry of Education, College of Science, Harbin Engineering University, Harbin 150001, China

Yuliya Semenova
Technological University Dublin, yuliya.semenova@tudublin.ie

Follow this and additional works at: https://arrow.tudublin.ie/engscheleart2
See next page for additional authors

Part of the Optics Commons, and the Other Electrical and Computer Engineering Commons

Recommended Citation

Wang, P. et al. (2014) Photonic crystal fiber half-taper probe based refractometer. Optics Letters, Vol. 39, No. 7, pp. 2076-2079, 2014. doi:10.1364/OL.39.002076

This Article is brought to you for free and open access by the School of Electrical and Electronic Engineering at ARROW@TU Dublin. It has been accepted for inclusion in Articles by an authorized administrator of ARROW@TU Dublin. For more information, please contact yvonne.desmond@tudublin.ie, arrow.admin@tudublin.ie, brian.widdis@tudublin.ie.

This work is licensed under a Creative Commons Attribution-Noncommercial-Share Alike 3.0 License

Authors

Pengfei Wang, Ming Ding, Lin Bo, Chunying Guan, Yuliya Semenova, Weimin Sun, Libo Yuan, Gilberto Brambilla, and Gerald Farrell

This article is available at ARROW@TU Dublin: https://arrow.tudublin.ie/engscheleart2/103

A photonic crystal fiber half taper probe based refractometer

Pengfei Wang[1,2*] Ming Ding[2], Lin Bo[1], Chunying Guan[3], Yuliya Semenova[1], Weimin Sun[3], Libo Yuan[3], Gilberto Brambilla[2] and Gerald Farrell[1,3]

[1]Photonics Research Centre, Dublin Institute of Technology, Kevin Street, Dublin 8, Ireland
[2]Optoelectronics Research Centre, University of Southampton, Southampton SO17 1BJ, United Kingdom
[3]Key laboratory of In-fiber Integrated Optics of Ministry of Education, College of Science, Harbin Engineering University, Harbin 150001, China
**Corresponding author: pengfei.wang@dit.ie*

Abstract: A compact singlemode - photonic crystal fibre - singlemode fibre tip (SPST) refractive index sensor is demonstrated in this paper. A CO_2 laser cleaving technique is utilsed to provide a clean-cut fibre tip which is then coated by a layer of gold to increase reflection. An average sensitivity of 39.1 nm/RIU and a resolvable index change of 2.56×10^{-4} are obtained experimentally with a ~3.2 μm diameter SPST. The temperature dependence of this fiber optic sensor probe is presented. The proposed SPST refractometer is also significantly less sensitive to temperature and an experimental demonstration of this reduced sensitivity is presented in the paper. Because of its compactness, ease of fabrication, linear response, low temperature dependency, high sensitivity, easy connectivity to other fibreized optical components and low cost, this refractometer could find various applications in chemical and biological sensing.
OCIS Codes: 060.2310, 060.2370, 060.5295

Optical fibre based photonic devices have been successfully used in a range of sensing applications. To date they have offered numerous advantages over conventional electrical sensors due to their immunity to electromagnetic interference, resistance to erosion, small size, high sensitivity and capability of remote sensing. In the past few years, several types of refractive index (RI) optical fibre sensors have been developed. The most common approaches rely on fibre Bragg gratings (FBGs) [1,2], long period gratings (LPGs) [3,4], microbending [5], Fabry-Perot interferometers [6,7], and microfibre coil resonators [8]. However, most of them require expensive fibres or equipment to produce.

An inexpensive singlemode-multimode-singlemode (SMS) fibre based sensor utilizing multimode interference in the multimode fibre (MMF) core section has been proposed [9-12]. This SMS fibre based refractive index sensor reported in [12] allows for the measurement of the external refractive index with a maximum sensitivity of 1815 nm/RIU (refractive index unit) and a dynamic range of 0.095 from 1.342 to 1.437. However given the fact that a long portion of an MMF needs to be etched chemically and also must be exposed to the surrounding medium in order to achieve a large refractive index change, the length of the MMF in the SMS structure is required to be sufficiently long, which makes it difficult to implement a compact probe type sensor with good spatial resolution. For example, in order to obtain a maximum sensitivity of 1815 nm/RIU, experimentally the diameter of the MMF part needs to be etched down to 80 μm and the length of the MMF must to be controlled accurately to 42 mm, but this increases the risk of breakage and difficulty. On the other hand, the high temperature dependence of the SMS structure significantly influences the refractive index measurement and additional temperature compensation is essentially needed.

Recently significant effort has been devoted to develop fibre devices with a range of advantages such as a large evanescent field, strong confinement, smart footprint, compact physical size and fast response. One approach to achieving these requirements is fibre tapering, which offers the potential to both improve the performance and to reduce the physical size of the SMS structure based fibre sensor mentioned above. In [13] we have presented a singlemode - periodically tapered photonic crystal fibre (PCF) - singlemode fibre structure based refractive index sensor with a high refractive index sensitivity combined with a low temperature dependence. To further develop this hybrid structure into a fibre probe sensor capable to perform a spatial resolved sensing, in this paper, a compact fibre refractometer based on a PCF half taper probe is presented. In both the conical transition region and the fiber tip sections, modal propagation (and thus multimode interference) depends on the external refractive index changes, therefore the PCF tip can be potentially used as a highly sensitive refractive index sensor with a high spatial resolution.

A refractometer based on a tapered photonic crystal fiber (PCF) tip terminated with a solid silica-sphere has been previously reported [14]. This was fabricated by splicing one end of the holey PCF to a singlemode fiber (SMF) and applying an electric arc at the other end to form a solid sphere. The difference between the work presented in this letter and previous work on PCF tip in [14] is that we have used a CO_2 laser for simply cleaving the solid core PCF (LMA-8, NKT Photonics, Denmark) directly and then form a PCF half taper due to the thermal effects. Because of the multimode interference in the half tapered PCF tip structure, the reflective spectrum of the hybrid device is strongly dependent on the spatial filtering of the input/output SMF.

The schematic configuration of the PCF tip used in the experiments is shown in Fig. 1: the fibre structure under consideration consists of an input/output SMF, a PCF half taper section and a gold film at the end of the fibre tip acting as a mirror.

Figure 2 shows the schematic of the experimental setup used to fabricate the PCF half taper. First a low-loss SMF-PCF-SMF (SPS) device was fabricated from the PCF (length circa 40 mm) sandwiched between two standard SMF28 optical fibres using a conventional fusion splicer. As shown in Fig. 2, a CO_2 laser (SYNRAD, Model: 48-2KWL) with a maximum power 30 W at the wavelength λ=10.6 μm was employed to fabricate the PCF half taper. A ZnSe cylindrical lens with a focal length of 254 ±0.5% mm focused the CO_2 laser beam width to ~150 μm. The SPS fibre device was fixed vertically on a support and a weight (~50 g) was used to apply a constant tension to the end of the SMF. When the middle of the PCF section was exposed to the CO_2 laser beam with an average output power of 15 W, tapering occurred because of heating and the tension applied to the fibre end by the weight. The waist of tapered fibre broke due to the heat accumulated of the CO_2 laser. Fig. 3 shows that the PCF tip has a diameter of circa 3.2 μm and a smooth tip surface. In order to improve reflectivity, the tip of the device was then coated with a gold film with a thickness of circa 40 nm, using a thermal evaporator. After that, the gold film from the long waist of the PCF and the conical transition region has been partially removed by carefully dropping a gold-etching solvent which contains iodine and potassium iodine solution, therefore only a thin gold film was left on the surface of PCF tip sample.

The reflection spectrum of the CO_2 laser cleaved, gold-coated SPS tip sample in air in the wavelength range from λ=1200 nm to 1600 nm is shown in Figure 4. As expected, several dips appear across the reflection spectrum, resulting from multimode interference in the PCF half taper. The reflectivity dips show an extinction ratio >10 dB. It is worth noting that as future work, we expect to fabricate a better SPS tip sample with Focus Ion Beam (FIB) milling and gold coating process, therefore the reflectivity can be improved and the refractive index measurement accuracy can be increased as a result.

The refractive index sensing measurement was performed at a room temperature (~25°C) with a series of calibrated RI liquids (1.33~1.38 with an interval of 0.005, RI error ±0.0002). The measurement set-up is shown in Fig. 5. A supercontinuum (SC) source (Fianium Ltd, Hamble, U.K.) was used to deliver light over a broad range of wavelengths (450 nm-1800 nm) with maximum pulse energy of 50 nJ. To protect the SC source, the fiberized output was angle-cleaved to avoid back reflections from the optical components. The SPS tip was inserted into each RI liquid in turn and the reflection spectrum from the SPST was recorded for each RI value by an optical spectrum analyzer (OSA) (Yokogawa, AQ6317, Japan) via an optical circulator.

Figure 6(a) shows the spectral shift of the peak at ~1546 nm for refractive indices increasing from 1.33 to 1.36. As the RI increases, the spectrum shows a redshift. The dip wavelength shift as a function of RI and the corresponding linear fit are presented in Figure 6(b). An average sensitivity of circa 39.1 nm/RIU over an RI range of 1.33~1.38 is achieved, resulting in a resolvable index change of 2.56×10^{-4} for a resolvable wavelength change of 10 pm. A higher sensitivity based on this hybrid fibre probe will be achieved in the near future by either optimizing the profile of the SPST or nanofabricating the PCF tip.

To study the temperature dependence of the SPST, the sample is placed on a thermoelectric cooler (TEC) as shown in Fig. 7. The temperature of the TEC element is controlled by a temperature controller. A thermistor is used to provide temperature feedback to the controller from the TEC element. An additional handheld thermometer is used to confirm the temperature on the TEC surface. The entire setup is placed inside a controlled small environmental chamber. For the purpose of this experiment the ambient temperature inside the chamber is fixed at 20°C as a starting point.

Since the PCF is composed of only fused silica, it is expected to have minimal thermal sensitivity. To determine the temperature dependence of the device the interference peak shift is observed while varying the temperature of the device from 20°C to 80°C.

Fig. 8 shows this temperature dependence for the SPST device. When the temperature is incremented from 20°C to 80°C the interference peak exhibits minute shifts to longer wavelengths. As expected the thermal sensitivity of the SPST is very low, confirmed by the thermal sensitivity obtained in the experiment for the SPST device which is circa 7.67 pm/°C.

In conclusion, a compact refractometer which uses a CO_2 laser cleaved and gold-coated SPST has been demonstrated. The refractometer has an experimentally confirmed average sensitivity of 39.1 nm/RIU and a resolvable index change of 2.56×10^{-4} for a resolvable wavelength change of 0.01 nm, with a ~3.2 μm diameter SPST. A very small temperature dependence of circa 7.67 pm/°C for this fiber structure has also been demonstrated. The sensitivity can be improved either by optimizing the profile of the SPST or by nanofabricating the PCF tip. This fibre sensor offers several advantages, including compact size which would allow for a good spatial resolution, but also ease of fabrication, a linear response, high sensitivity, low temperature dependence, ease of interconnection with other fiberized optical components and low cost. This device is a promising candidate for sensing in various chemical and biological applications.

P. Wang is funded by the Royal Irish Academy Mobility Fellowship 2013. L. Bo would like to thank the International Centre for Graduate Education in micro & nano Engineering (ICGEE) and the IRC for her Ph.D. funding support. G. Brambilla gratefully acknowledges the Royal Society (London) for his university research fellowship. This work was supported by the 111 project (B13015), at the Harbin Engineering University. This publication has emanated from activity supported in part by Science Foundation Ireland (SFI) under the International Strategic Cooperation Award Grant Number SFI/13/ISCA/2845.

References

1. M. Han, F. W. Guo, and Y. F. Lu, Optics Letters, 35, 399 (2010).
2. H. Y. Meng, W. Shen, G. B. Zhang, C. H. Tan, and X. G. Huang, Sensors and Actuators B-Chemical, 150, 226 (2010).

3. J. L. Li, W. G. Zhang, S. C. Gao, P. C. Geng, X. L. Xue, Z. Y. Bai, and H. Liang, IEEE Photonics Technology Letters, 25, 888 (2013).
4. Q. Han, X. W. Lan, J. Huang, A. Kaur, T. Wei, Z. Gao, and H. Xiao, IEEE Photonics Technology Letters, 24, 1130 (2012).
5. H. M. Liang, H. Miranto, N. Granqvist, J. W. Sadowski, T. Viitala, B. C. Wang, and M. Yliperttula, Sensors and Actuators B-Chemical, 149, 212 (2010).
6. O. Frazao, P. Caldas, J. L. Santos, P. V. S. Marques, C. Turck, D. J. Lougnot, and O. Soppera, Optics Letters, 34, 2474 (2009).
7. J. L. Kou, J. Feng, Q. J. Wang, F. Xu, and Y. Q. Lu, Optics Letters, 35, 2308 (2010).
8. F. Xu and G. Brambilla, Applied Physics Letters, 92, 101126 (2008).
9. P. Wang, G. Brambilla, M. Ding, Y. Semenova, Q. Wu, G. Farrell, Optics Letters, 36, 2233 (2011).
10. P. Wang, G. Brambilla, M. Ding, T. Lee, L. Bo, Y. Semenova, Q. Wu, G. Farrell, IEEE Sensors Journal, 13, 180 (2013).
11. P. Wang, G. Brambilla, M. Ding, Y. Semenova, Q. Wu, G. Farrell, Journal Optical Society of America B, 28, 1180 (2011).
12. Q. Wu, Y. Semenova, P. Wang and G. Farrell, Optics Express, 19, 7937 (2011).
13. P. Wang, L. Bo, C. Guan, Y. Semenova, Q. Wu, G. Brambilla and G. Farrell, Optics Letters, 38, 3795 (2013).
14. K. Mileńko, D. Hu, P. Shum, T. Zhang, J. Lim, Y. Wang, T. Woliński, H. Wei, and W. Tong, Optics Letters, 37, 1373 (2012).

Figure captions

Figure 1. Schematic of the proposed PCF half taper sensor.

Figure 2. Schematic of the experimental setup for fabricating a PCF half taper.

Figure 3. Microscope image of (a) the PCF tip and (b) zoomed image of the PCF tip.

Figure 4. Reflectivity of the SPS half taper in air after CO2 laser cleaving and gold coating process.

Figure 5. Experimental set-up for refractive index measurement.

Figure 6 (a) Spectral shift of the peak at ~1546 nm for an RI increasing from 1.33 to 1.36; (b) The wavelength shift of the peak as a function of RI.

Figure 7. Experimental setup to study the temperature stability of the SPST.

Figure 8. Temperature dependence of the reflectivity of the SPST device.

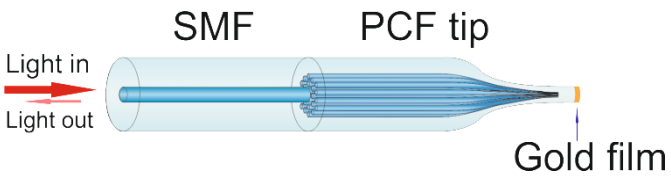

Figure 1.

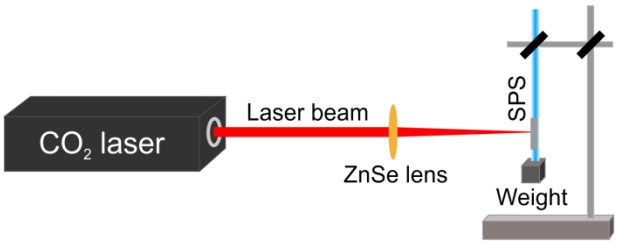

Figure 2.

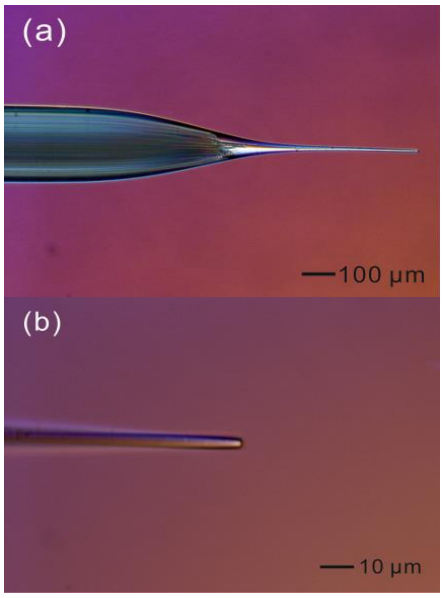

Figure 3.

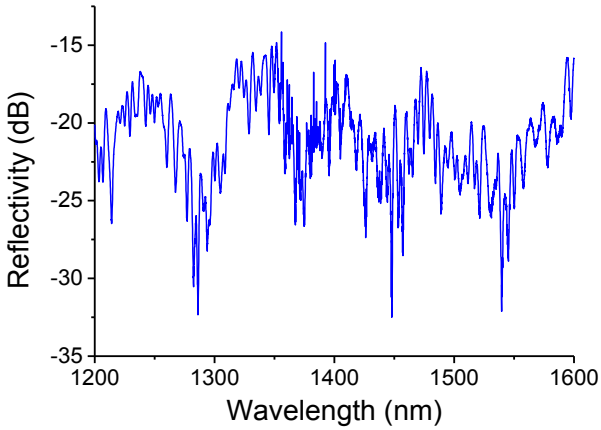
Reflectivity (dB)
-15
-20
-25
-30
-35
1200
1300
1400
1500
1600
Wavelength (nm)

Figure 4.

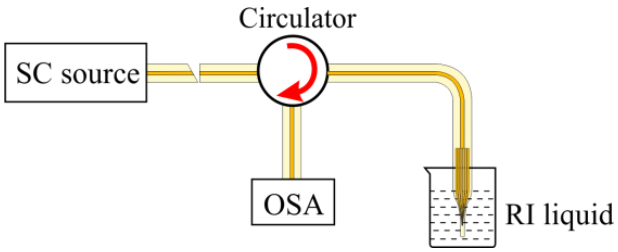

Figure 5.

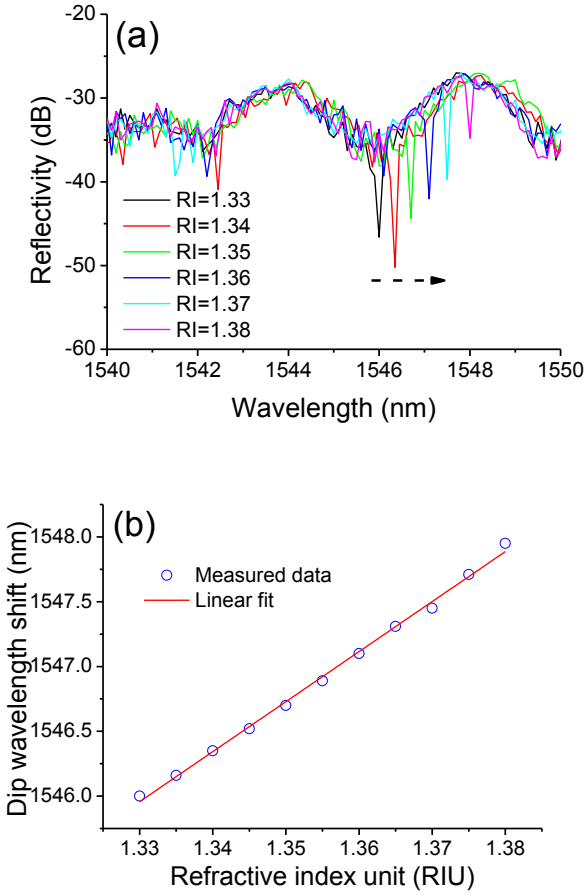
(a)
Reflectivity (dB)
-20
-30
-40
-50
-60
RI=1.33
RI=1.34
RI=1.35
RI=1.36
RI=1.37
RI=1.38
1540
1542
1544
1546
1548
1550
Wavelength (nm)
(b)
Dip wavelength shift (nm)
1548.0
1547.5
1547.0
1546.5
1546.0
Measured data
Linear fit
1.33
1.34
1.35
1.36
1.37
1.38
Refractive index unit (RIU)

Figure 6. (a), (b)

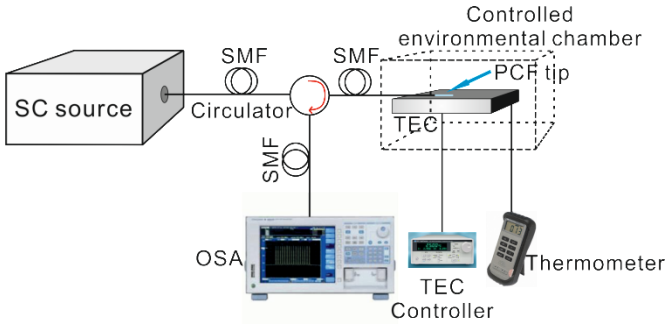
Controlled
environmental chamber
SC source
SMF
SMF
Circulator
PCF tip
TEC
SMF
OSA
TEC
Controller
Thermometer

Figure 7.

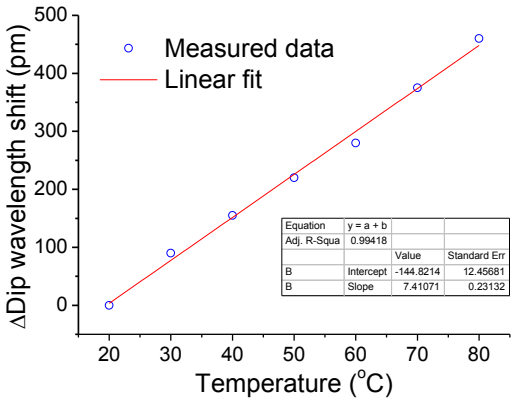
Measured data
Linear fit
ΔDip wavelength shift (pm)
Temperature (°C)
500
400
300
200
100
0
20
30
40
50
60
70
80
Equation y = a + b
Adj. R-Squa 0.99418
Value Standard Err
B Intercept -144.8214 12.45681
B Slope 7.41071 0.23132

Figure 8.